Chemical Engineering Journal 220 (2013) 89–97

Contents lists available at SciVerse ScienceDirect

Chemical Engineering Journal

journal homepage: www.elsevier.com/locate/cej

Separation of ethanol–water liquid mixtures by adsorption on a polymeric resin Sepabeads 207®

J.A. Delgado, V.I. Águeda, M.A. Uguina, J.L. Sotelo, A. García, P. Brea, A. García-Sanz *

Chemical Engineering Department, Complutense University of Madrid, 28040 Madrid, Spain

HIGHLIGHTS

- Ethanol and water capacities, and mass transfer coefficients have been determined.
- A multi-column cyclic adsorption–desorption process has been designed.
- Estimated net ethanol product is higher for Sepabeads 207 resin than for silicalite.

ARTICLE INFO

Article history:
Received 26 November 2012
Received in revised form 14 January 2013
Accepted 16 January 2013
Available online 26 January 2013

Keywords:
Ethanol–water mixtures
Polymeric resin
Modelling
Cyclic adsorption–desorption process

ABSTRACT

Production of alcohol by fermentation of renewable resources like plant biomass is becoming an effective method for increasing liquid clean fuel production. Hence, ethanol recovery from fermentation broths is of huge interest. The process here studied is the separation of ethanol–water mixtures by adsorption on a polymeric resin (Sepabeads 207®). The column capacities of ethanol and water as a function of liquid composition have been determined, together with the mass transfer parameters. A theoretical model for predicting the column dynamics in this system has been developed, considering the effect of mass transfer resistance in the full concentration range (between 0% and 100% ethanol). The model, based on conservation equations, has been validated with experimental data obtained in a laboratory column. It has been also applied to design a multi-column cyclic adsorption–desorption process for separating a 10% ethanol–water mixture using the polymeric resin Sepabeads 207® as adsorbent. The net ethanol product obtained is higher than using silicalite as adsorbent.

1. Introduction

Bioethanol is one of the most promising liquid clean fuels which are of huge interest nowadays [1–5]. The conventional technology for producing bioethanol, based on distillation to separate the ethanol from the fermentation mixture, is very energy-intensive, because the ethanol–water azeotrope (95.6% w/w ethanol) must be broken. Several alternatives to the distillation of ethanol–water mixtures have been proposed, including ethanol extraction with CO_2 [6], solvent extraction [7,8], adsorption-based processes [9–13], or a combination of extraction with CO_2 and adsorption processes [14], and pervaporation [15–17]. Among them, adsorption processes appear very interesting, since ethanol and water molecules differ in size and have different dipole moment [18]. Adsorption based processes are rather promising to reduce significantly the energy for this separation [19]. Pitt et al. [10] proposed an adsorption process to recover ethanol from fermentation broths (ethanol concentration up to 10% w/w) based on the adsorption of ethanol on hydrophobic sorbents. Some examples of hydrophobic adsorbents suitable for the recovery of alcohols are activated coconut charcoal, carbon molecular sieves, divinylbenzene cross-linked polystyrene beads and high silica hydrophobic molecular sieves, such as ZSM-5 and silicalite [20]. After the adsorption step the column was regenerated by purging with hot air, recovering the desorbed ethanol by condensation. Later, Sircar and Rao [21,22] patented two cyclic multi-column adsorption processes for the separation of bulk liquid mixtures (concentration swing adsorption, CSA, and concentration thermal swing adsorption, CTSA) which can be used in the ethanol–water separation with ethanol-selective adsorbents.

Delgado et al. [23] proposed an adsorption separation process using silicalite, based on the one suggested by Pitt et al. [10]. Water is removed from the column after the adsorption step by rinsing it with 100% ethanol. The reported process adds a new step, rinse recovery, which can give good results in terms of ethanol purity (>99.5%) and recovery (above 95%). This process only requires energy to desorb ethanol while purging the column with air. After the

* Corresponding author. Tel.: +34 913948511.
E-mail address: aliciagarcia@quim.ucm.es (A. García-Sanz).

1385-8947/$ - see front matter © 2013 Elsevier B.V. All rights reserved.
http://dx.doi.org/10.1016/j.cej.2013.01.057

Nomenclature

C_0	initial sodium chloride concentration in the column ($g\,l^{-1}$)
C_{out}	sodium chloride concentration in the outlet stream ($g\,l^{-1}$)
D_L	axial dispersion coefficient ($m^2\,s^{-1}$)
d_P	particle diameter (m)
F	mass flow rate ($kg\,s^{-1}$)
$k_{s,i}$	LDF global mass transfer coefficient ($m\,s^{-1}$)
L	bed length (m)
L_{MTZ}	mass transfer zone length (m)
MTZ	mass transfer zone
N_i	mass transfer rate between liquid phase and adsorbed homogeneous phase ($kg\,m_{bed}^{-3}\,s^{-1}$)
$n_i(y_i)$	column capacity measured at equilibrium $\left(kg\,kg_{adsorbent}^{-1}\right)$
$\bar{q}_i$	average solid-phase concentration $\left(kg\,kg_{adsorbent}^{-1}\right)$
q_i^*	concentration in the homogeneous solid-phase in equilibrium with the liquid filling the interstices $\left(kg\,kg_{adsorbent}^{-1}\right)$
Q_F	flow rate ($m^3\,s^{-1}$)
S	equilibrium selectivity, parameter defined in Eq. (23)
S_B	column section (m^2)
t	time (s)
T	temperature (K)
u_{MTZ}	velocity of the mass transfer zone ($m\,s^{-1}$)
V_B	parameter defined in Eq. (13) (m^3)
V_G	parameter defined in Eq. (13) (m^3)
V_H	parameter defined in Eq. (13) (m^3)
V_T	parameter defined in Eq. (13) (m^3)
V_V	parameter defined in Eq. (13) (m^3)
W	mass of adsorbent in the column (kg)
x_i	mass fraction in the liquid phase, parameter defined in Eq. (23)
Y_i	mass fraction in the adsorbed phase, parameter defined in Eq. (23)
y_i	mass fraction

Greek symbols

ρ	liquid density ($kg\,m^{-3}$)
ε	bed interparticle voidage fraction ($m_{void}^3 \cdot m_{bed}^{-3}$)
u	superficial velocity ($m\,s^{-1}$)
μ	liquid viscosity (Pa s)
ρ_P	particle density ($kg_{particle} \cdot m_{particle}^{-3}$)

Subscripts

0	initial column conditions
1	ethanol
2	water
atm	at atmospheric pressure
F	feed condition
i	ith component

study developed by Delgado et al. [24], the regeneration of a polymeric resin column (Sepabeads 207®) saturated with ethanol with air purge and external heating was possible at low temperature (35–36 °C), so waste heat can be used as a source of energy in this step. Moreover, as polymeric resins also adsorb ethanol from water at these temperatures [10], the cooling step between the adsorption and regeneration steps can be eliminated in the adsorption–regeneration cycle. Little information can be found in the literature about the separation of bulk ethanol–water mixtures with polymeric resins. For designing this separation process, the adsorption behavior in a wide concentration range (from the typical concentrations in fermentation broths up to pure ethanol) must be studied. Some authors have determined the isotherms in liquid phase for ethanol and water over silicalite-1 [23,25], modified ZSM-5 and β zeolite [25].

The objective of this work is to measure and to model the column dynamics in the separation of bulk liquid ethanol–water mixtures by adsorption with the polymeric resin Sepabeads 207®. The column capacities of ethanol and water have been determined from fixed bed experiments at different ethanol concentrations between 6% and 100% (w/w). To ensure that both adsorption and regeneration steps can be carried out at the same temperature, the adsorption experiments have been carried out at 35 °C. A theoretical model has been developed for predicting the column dynamics in this system, which has been validated with experimental data. The model has been used to design a cyclic adsorption–desorption process for separating an ethanol–water mixture with the proposed adsorbent. Although we have carried out a similar work using silicalite pellets as the adsorbent [23], this work contributes with the following new features, apart from the different adsorbent:

(a) The theoretical model describing the column dynamics of a bulk liquid ethanol–water separation has been adapted to a system where it is not possible to distinguish between the adsorbed phase and liquid phase in the column. In our previous work, the liquid phase fills the voids between pellets and the pellet macropores, and the adsorbed phase fills the silicalite micropores.
(b) The designed cyclic separation process has been improved to handle the case when the mass transfer zone length of the adsorption step is significant. This was not the case for silicalite.
(c) A new method is proposed for calculating the net ethanol product of the separation process (in kg of ethanol product/kg of adsorbent) when the liquid and the adsorbed phases are not distinguishable, as it happens with Sepabeads 207®.

2. Materials and methods

Absolute ethanol (>99.5% v/v) was purchased from Panreac® (Spain). Water was obtained from a Milli-Q purifier (Millipore®). The adsorbent used in this work (Sepabeads 207®) is a commercial polymeric resin with a poly(styrenedivinylbenzene) matrix. The properties of this adsorbent, including the bed properties in the experiments with a column 0.1 m long, are given in Table 1.

The experimental setup is shown in Fig. 1. It consists of an aluminum column loaded with the adsorbent, resting on an analytical balance (1 mg – 310 g weighing range) connected online to a

Table 1
Adsorbent and bed properties (Sepabeads 207®).

Particle density	650 $kg\,m^{-3}$
Average particle size	350 μm
BET surface	600 $m^2\,g^{-1}$
Pore volume (from Hg porosimetry)	0.93 $cm^3\,g^{-1}$
Bed length	0.1 m
Bed diameter	0.0105 m
Adsorbent weight	3.329 g
Bed interparticle voidage fraction	0.407

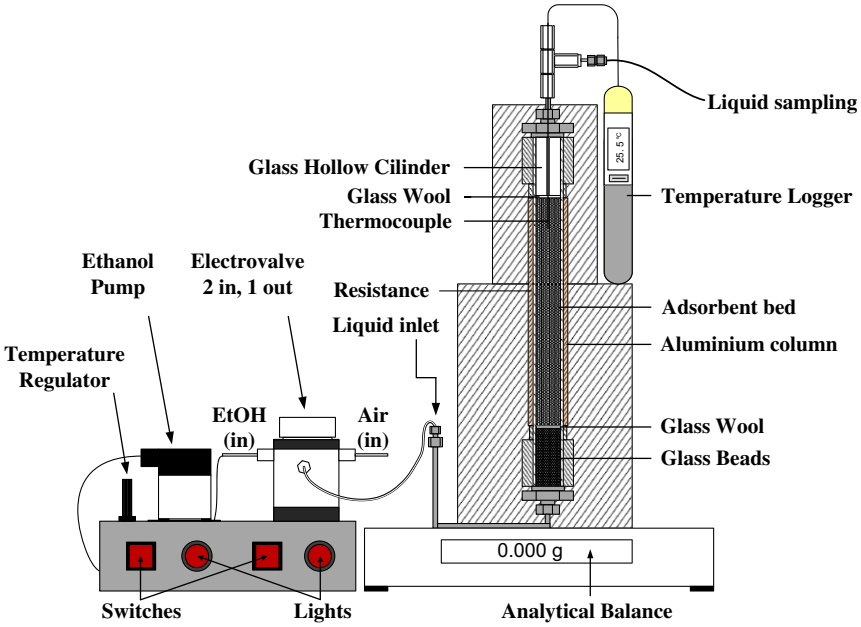

Fig. 1. Picture of the experimental set-up.

computer. Upward flow is used to facilitate the removal of air from the column. The column is covered with a Kapton® heater to change the bed temperature, which is registered in a temperature logger. The thermocouple tip of this device is located at 1 cm from the bed end. The heat supply given by the heater is changed with a potentiometer. The bed is connected to the fluid supply (liquid or gas) with a 1/16" Teflon® tube. The total weight resting on the balance was about 250 g, which was high enough to make the interference of the connecting tube and the heater wires unnoticeable.

The column is fed from the bottom part. The ethanol concentration of the outlet stream (top part of the column) is measured using a RI (Refraction Index) detector. In the experiment with aqueous sodium chloride to measure the void volume, the sodium chloride concentration is measured with a conductivity detector.

Three kinds of experiments were performed with this installation:

(a) Column capacity measurement experiments of ethanol and water on the polymeric resin.
(b) Ethanol desorption experiments with water.
(c) Rinse experiments with pure ethanol.

Before each experiment, the heat supply to the column is fixed with the potentiometer, to reach a bed temperature of 35 °C. To regenerate the column, except for the desorption experiments with water, it is purged with air keeping the heat supply until the weight loss stops.

In the column capacity measurement experiments, an ethanol–water liquid mixture with a pre-established concentration is fed into the empty column (filled with resin and air) with a HPLC pump. The feed flow rate remains constant at 1 ml min^{-1}. The bed weight evolution and temperature are recorded. The experiments are conducted until the ethanol concentration in the outlet stream is equal to the one of the feed stream.

In the desorption experiments with water, the column is previously saturated with an ethanol–water mixture with a pre-established composition. Then, Milli-Q water (1 ml min^{-1}) is fed to desorb and displace the ethanol in the column. When no ethanol is measured in the outlet stream the experiment is stopped.

Prior to the rinse experiments, the column is filled with a 10% w/w ethanol–water mixture. To rinse the column, pure ethanol is fed at a constant rate of 1 ml min^{-1}. The experiment finishes when pure ethanol comes out of the column and thus, all the water has been removed.

3. Theoretical model

The measurement and interpretation of the adsorption of a bulk liquid mixture on a solid adsorbent presents important difficulties because the density of the adsorbed phase is similar to the one of the bulk fluid, and the density of the adsorbed phase is not open to direct measurement [20]. Thus, it is not possible to separate the amounts of adsorbed and non-adsorbed phases in the system without introducing any assumption. This problem is accentuated if the adsorbent is a polymeric resin, where both adsorption on the internal surface of the resin, and absorption (penetration of the adsorbate in the polymeric matrix) can occur. When working with the adsorption of a bulk liquid mixture on a packed bed of adsorbent, the only amount which can be measured experimentally is the total column capacity for each component, including both adsorbed and non-adsorbed amounts. In this work, the assumption considered is that the total column capacity is divided into two zones: (1) voids between the resin beads, (2) pore volume inside the beads plus the volume of dense polymeric matrix. The volume of zone 1 is calculated as the bed interparticle voidage fraction times the column volume. The interphase between the two zones is the external surface of the resin beads. The masses of ethanol and water filling the column are distributed among the two zones described previously. The ethanol–water mixture filling zone 1 has the properties of a liquid mixture, so the component concentration in zone 1 is the liquid density times the corresponding mass fraction. The mixture filling zone 2 is assumed to be a homogeneous solid-phase for simplicity. The amounts of ethanol and water filling zone 2 at equilibrium are calculated by subtracting the mass of each component in zone 1 from the column capacity measured experimentally for each component at equilibrium. The component concentration in zone 2 is calculated as the mass of each component in this zone divided into the mass of resin. The phases in zones 1 and 2 will be

called liquid phase and homogeneous solid-phase, respectively, from now on.

On this basis, the theoretical model for describing the column adsorption dynamics is derived from mass and momentum balances, based on the following additional assumptions:

(i) The system is isothermal.
(ii) The mobile phase is described by an axial-dispersed plug flow model. The mobile phase only moves in zone 1.
(iii) The rate of mass transfer of each component between liquid and homogeneous solid-phase is given by a linear driving force (LDF) expression. The driving force is the concentration in the homogeneous solid-phase in equilibrium with the liquid in contact with the solid-phase minus the concentration in the homogeneous solid-phase.

The total mass balance in a differential portion of the column is described by (1 = ethanol, 2 = water):

$$\varepsilon\frac{\partial\rho}{\partial t} = -\frac{\partial(u\rho)}{\partial z} - \left(\sum_{i=1}^{i=2} N_i\right) \tag{1}$$

where ρ is the liquid density, t is time, ε is the bed interparticle voidage fraction, u is the superficial velocity, z is the axial coordinate, and N_i is the mass transfer rate of the ith component between liquid phase and adsorbed homogeneous phase.

The effect of the composition on the liquid density is described with the following empirical equation, which was obtained by fitting the experimental data available in Perry's handbook [26] for ethanol–water mixtures:

$$\rho(y_i, 1\ \text{atm}) = \frac{\rho_1 y_1}{1 - a y_2} + \frac{\rho_2 y_2}{1 - a y_1} \tag{2}$$

where y_i is the mass fraction of each component. At 35 °C and 1 bar, ρ_1 = 776 kg m^{-3}, ρ_2 = 994 kg m^{-3}, a = 0.03723.

An equation of state is required get a relationship between the time-derivatives of pressure and density. The following equation of state is proposed, assuming that the derivative of density with respect to pressure is constant at constant temperature for a small pressure change:

$$\rho(y_i, P) = \rho(y_i, P_{atm}) + \left.\frac{\partial\rho}{\partial P}\right|_T (P - P_{atm}) \tag{3}$$

The value of $\partial\rho/\partial|_T$ was taken as 3.7×10^{-7} kg m^{-3} Pa^{-1}, estimated for pure water at 25 °C in the pressure range from 1 to 25 bar [27]. This parameter has little effect on the simulated results when changed by a factor of 10, so it is not necessary to use an accurate value in the simulation. The time-derivative of pressure at any axial point can be estimated from Eq. (1) as:

$$\frac{\partial P}{\partial t} = \frac{\partial\rho/\partial t - \sum_{i=1}^{i=2}(\partial\rho/\partial y_i)(\partial y_i/\partial t)}{\partial\rho/\partial P|_T} \tag{4}$$

The superficial velocity is related to the pressure gradient according to Ergun's equation:

$$-\frac{\partial P}{\partial z} = \frac{150\mu(1-\varepsilon)^2}{\varepsilon^2 d_p^2}u + \frac{1.75(1-\varepsilon)\rho}{\varepsilon^2 d_p}u^2 \tag{5}$$

where μ is the liquid viscosity, and d_P is the particle diameter.The mass transfer rate between liquid and solid-phase for each component is given by:

$$N_i = (1-\varepsilon)\rho_p\frac{\partial\overline{q_i}}{\partial t} \tag{6}$$

where ρ_P is the particle density. Eq. (6) can be simplified to Eq. (7) with the LDF approximation:

$$N_i = (1-\varepsilon)\rho_p k_{s,i}(q_i^* - \overline{q_i}) \tag{7}$$

where $k_{s,i}$ is the LDF global mass transfer coefficient of the ith component, q_i^* is the concentration in the homogeneous solid-phase $\left(\text{kg}_i\ \text{kg}_{\text{adsorbent}}^{-1}\right)$, in equilibrium with the liquid filling the interstices and $\overline{q_i}$ is the average solid-phase concentration. The value of q_i^* are calculated by subtracting the amount of the ith component in the liquid phase from the column capacity measured experimentally at equilibrium ($n_i(y_i)$):

$$q_i^* = n_i(y_i) - \frac{\rho y_i \varepsilon}{(1-\varepsilon)\rho_p} \tag{8}$$

The mass balance for each component in a differential portion of the column gives the variation of the corresponding weight fraction with time:

$$\frac{\partial y_i}{\partial t} = \frac{D_L}{\rho}\frac{\partial\rho}{\partial z}\frac{\partial y_i}{\partial z} + D_L\frac{\partial^2 y_i}{\partial z^2} - \frac{u}{\varepsilon}\frac{\partial y_i}{\partial z} - \frac{N_i}{\varepsilon\rho} + \frac{\left(\sum_{i=1}^{i=2} N_i\right)y_i}{\varepsilon\rho} \tag{9}$$

where D_L is the axial dispersion coefficient.

The boundary conditions giving the time dependence of P and y_i at z = 0 and z = L, where L is the bed length, are the following:

$$z = 0 \quad u\rho = \frac{Q_F}{S_B}\rho_F \quad z = L \quad P = P_{atm} \tag{10}$$

$$z = 0 - \varepsilon D_L\frac{\partial y_i}{\partial z} + u(y_i - y_{i,F}) = 0 \quad z = L \quad \frac{\partial y_i}{\partial z} = 0 \tag{11}$$

where Q_F is the feed flow rate, S_B is the column section, and the subscript F indicates feed conditions. The initial values of the dependent variables are:

$$t = 0 \quad \forall z,\ P = P_{atm};\ y_i = y_{i,0};\ \overline{q_i} = q_i^*(y_{i,0}) \tag{12}$$

where the subscript 0 indicates the initial column conditions.

The complete model was solved numerically using the PDECOL package, a public domain code for research purposes developed by Madsen and Sincovec [28] which uses orthogonal collocation on finite elements technique. This package is based on the method of lines and uses a finite element collocation procedure (with piecewise polynomials as the trial space) for the discretization of the dimensionless spatial variable z. The collocation procedure reduces the PDE system to a semi-discrete system which then depends only on the time variable t.

The fitting quality of the models was evaluated by calculating the coefficient of determination (r^2), which is defined as:

$$r^2 = 1 - \sum_1^n (y_{calc} - y_{exp})^2 / \sum_1^n (y_{exp} - \overline{y_{exp}})^2 \tag{13}$$

where n is the number of experimental points and y is the regressed variable. The statistical significance of the regressed parameters was evaluated by calculating their 95% confidence intervals. For the parameters in the algebraic models (Eqs. (21) and (22)), the 95% confidence intervals were calculated with the Origin 6.0® program. For the parameters in the dynamic differential model (Eqs. (1)–(12)), the 95% confidence intervals were calculated following the method proposed by Froment and Bischoff for models that are non-linear in the parameters [29].

4. Results and discussion

4.1. Determination of the void volume and the axial dispersion coefficient

In order to describe the adsorption dynamics of ethanol–water mixtures on the polymeric resin column, as well as to measure the column capacities of ethanol and water, the void volume in the installation must be known. The total void volume (V_V) includes

the void volume in the following zones: connecting tubes (V_T), a 5 cm long bed packed with glass beads before the adsorbent column (V_G), the 10 cm long resin bed (excluding the internal adsorbent porosity, already considered in the homogeneous solid-phase) (V_B), and a glass hollow cylinder 5 cm long after the bed (V_H). Therefore:

$$V_V = V_T + V_G + V_B + V_H \quad (14)$$

The total void volume was estimated with the column packed with glass beads (15 cm of glass beads and 5 cm of glass hollow cylinder). The glass beads are of the same size as the resin beads. The column was initially filled with a sodium chloride solution, and it was purged with water. The sodium chloride displacement curve obtained is shown in Fig. 2. The total void volume was calculated as:

$$V_V = Q_F \int_0^{t_\infty} \frac{C_{out}}{C_0} dt \quad (15)$$

where C_{out} is the sodium chloride concentration, resulting in $V_V = 7.77 \times 10^{-6}$ m^3. The void volume outside the resin bed is estimated as:

$$V_T + V_G + V_H = V_V - S_B L_B \varepsilon = 4.24 \times 10^{-6} \text{ m}^3 \quad (16)$$

where $L_B = 0.1$ m. The apparent dispersion coefficient in the installation (D_L) was estimated by fitting the model to the experimental sodium chloride displacement curve (Fig. 2), setting $N_i = 0$ in Eq. (7). It was assumed that dispersion only occurs in the zones filled with beads ($V_G + V_B$), whereas the flow pattern in V_T and V_H is plug flow. Thus, V_T and V_H only cause a delay time in the displacement curve:

$$t_D = \frac{V_T + V_H}{Q_F} = \frac{V_V - S_B(L_B + L_G)\varepsilon}{Q_F} \quad (17)$$

where $L_B + L_G = 0.15$ m. The estimated value of D_L was $(3.97 \pm 1.38)\,10^{-6}$ m^2 s^{-1}, with $r^2 = 0.99$. A comparison between the theoretical and the experimental displacement curve is presented in Fig. 2.

4.2. Measurement of ethanol and water column capacities

Several column capacity measurement experiments with liquid ethanol–water mixtures were carried out with different feed ethanol concentrations at 308 K. One experiment was carried out at 296 K to evaluate the effect of temperature on the column capacities. The feed ethanol concentrations studied are given in Table 2.

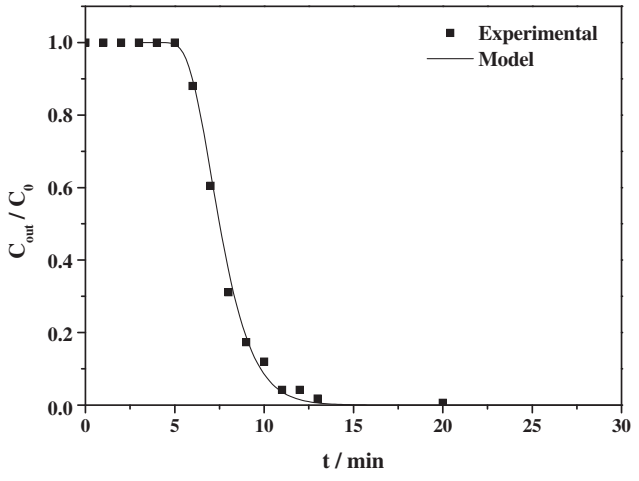

Fig. 2. Displacement curve of sodium chloride by water in the experimental installation packed with glass beads ($Q_F = 1$ ml min^{-1}, $C_0 = 8$ g l^{-1}). The line is obtained by fitting the model to the experimental data.

Table 2
Column capacities of ethanol (1) and water (2) and equilibrium selectivity towards ethanol for different liquid compositions.

$y_{1,F}$	T (K)	n_1 (kg kg$^{-1}_{adsorbent}$)	n_2 (kg kg$^{-1}_{adsorbent}$)	[a]$S_{1,2}$
0.06	308	0.12	0.92	2.32
0.08	308	0.16	0.94	2.20
0.10	308	0.19	0.91	2.11
0.10	308	0.22	0.88	2.11
0.10	296	0.20	0.80	–
0.20	308	0.36	0.85	1.84
0.20	308	0.44	0.71	1.84
0.30	308	0.47	0.64	1.69
0.30	308	0.50	0.73	1.69
0.40	308	0.61	0.64	1.59
0.50	308	0.73	0.55	1.51
0.80	308	1.11	0.12	1.35
1.00	308	1.25	0.00	–

[a] This parameter was calculated introducing Eqs. (21) and (22) in Eq. (23).

The column capacities are estimated from a mass balance around the experimental installation. The ethanol capacity is calculated as:

$$n_1 = \frac{\int_0^{t_\infty} (Q_F \rho_F y_{1,F} - F_{out} y_{1,out}) dt - (V_T + V_G + V_H)\rho_F y_{1,F}}{W} \quad (18)$$

where F_{out} is the mass flow rate of the effluent, $y_{1,out}$ is its ethanol mass fraction, and W is the resin bed mass. The evolution of F_{out} can be calculated from the time derivative of the experimental column weight history (dW_{column}/dt (t)):

$$F_{out}(t) = Q_F \rho_F - \frac{dW_{column}}{dt}(t) \quad (19)$$

The column water capacity has been calculated as:

$$n_2 = \frac{\Delta W_{column} - \int_0^{t_\infty} (Q_F \rho_F y_{1,F} - F_{out} y_{1,out}) dt - (V_T + V_G + V_H)\rho_F y_{2,F}}{W} \quad (20)$$

where ΔW_{column} is the column weight variation between the beginning and the end of the experiment. The estimated values of column capacities are given in Table 2. It is observed that the effect of temperature is quite small between 296 and 308 K, as the variation is within the experimental error (8.68%, calculated as average relative standard deviation following the IUPAC Recommendations [30]). This result indicates that cooling the column before the adsorption

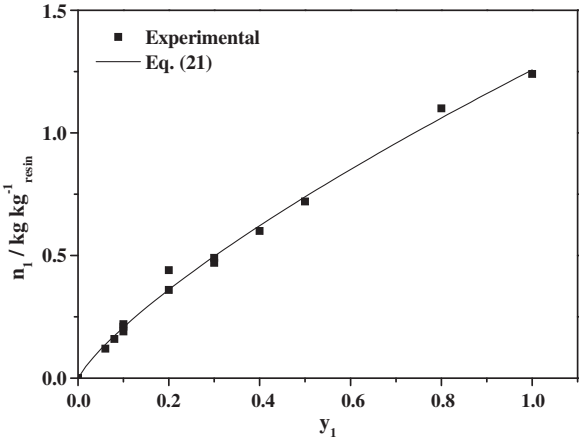

Fig. 3. Ethanol column capacity at 308 K for different liquid compositions.

step is not advantageous in the proposed process. The effect of the liquid composition on the column capacities at 308 K can be correlated with the following equations:

$$n_1 = \frac{3.8312 y_1}{1 + 2.0234 y_1^{0.3737}} \quad (21)$$

$$n_2 = 0.995 y_2 \quad (22)$$

These expressions were proposed because they gave a satisfactory reproduction of the experimental results. A comparison between the predicted and the experimental column capacities is shown in Figs. 3 and 4. Eqs. (21) and (22) were used to predict the column dynamics and to simulate the separation process, putting them into the theoretical model (in Eq. (8)). The values of r^2 for Eqs. (21) and (22) were 0.996 and 0.953 respectively. The 95% confidence interval of the parameter in Eq. (22) is ±0.05. The confidence intervals of the parameters in Eq. (21) were very large, indicating that many different combinations of model parameters lead to the same fitting quality. This was checked by setting a parameter in Eq. (21) to a different value and repeating the fitting procedure, keeping the parameter constant. An identical predicted curve (with practically the same value of r^2) was obtained, with a different combination of parameters ($n_1 = 6 \quad y_1/(1 + 3.72443\ y_1^{0.2992})$). It is important to note that, although the parameters in Eq. (21) have no statistical significance, a good reproduction of the experimental results is obtained if an appropriate combination of parameters is used.

The higher curvature of the plot of ethanol column capacity with respect to the one of water, as well as the higher ethanol capacities for the same mass fraction in the liquid, are indicative of the higher affinity of the resin towards ethanol. Moreover, this fact can be supported by the equilibrium selectivity towards ethanol ($S_{1,2}$) calculated with Eq. (23) according to Yang [31].

$$S_{1,2} = \frac{Y_1}{Y_2}\frac{x_2}{x_1} \quad (23)$$

where Y_i is the mass fraction of the two components in the adsorbed phase, whereas x_i is the corresponding mass fraction in the liquid phase. As the adsorbed amounts of each component are not available for the system studied in this work, Y_1 and Y_2 have been calculated using the column capacities (Eqs. (21) and (22)) instead of the adsorbed concentrations. The results are presented in Table 2, where it is observed that the selectivity towards ethanol is higher than 1 in all the concentration range, decreasing as the ethanol mass fraction in the liquid phase rises.

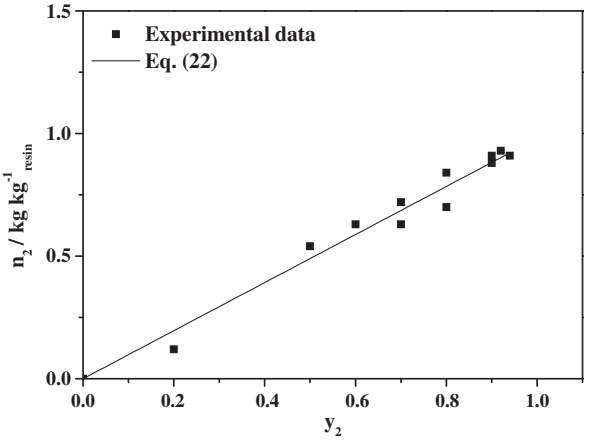

Fig. 4. Water column capacity at 308 K for different liquid compositions.

4.3. Estimation of the LDF mass transfer parameters

To model the column dynamics in the ethanol–water separation, once the column capacities and the bed properties are known, the only unknown parameters are the LDF mass transfer coefficients of ethanol and water, $k_{s,i}$ (Eq. (7)). Several ethanol desorption experiments (purging the column with water) starting from different initial ethanol concentrations were carried out, as described in the experimental section, in order to estimate the LDF mass transfer coefficients by nonlinear regression. Desorption experiments with water instead of adsorption experiments of ethanol–water mixtures were used for this purpose. As the adsorption of ethanol on a polymeric resin is of physical character (reversible), the mechanism of desorption is the same as the one of adsorption. We observed that in the adsorption experiments carried out to measure the column ethanol and water capacities, the first drops of liquid leaving the column come out mixed with air bubbles (the flow is not continuous for some time) and they have a quite high ethanol concentration (for a 50% ethanol feed was 42%). This indicates that the experimental column is not long enough to get an ethanol-free outlet stream. For this reason, it was not possible to obtain complete breakthrough curves covering the whole concentration range in these experiments, complicating the estimation of the mass transfer parameters.

The experimental results are presented in Fig. 5. The final average ethanol concentration in the recovered effluent (ethanol mixed with water) was not measured because desorption of ethanol with water does not take place in the separation process, where regeneration with air is proposed. Pure ethanol can be recovered by condensation. The air regeneration step of a Sepabeads 207® column loaded with 100% ethanol has already been studied elsewhere [24].

A sensitivity analysis was performed to determine the individual influence of the LDF parameters of ethanol and water on the simulated desorption curves, and it was observed that $k_{s,2}$ had very little effect with respect to that of $k_{s,1}$. In view of this, it was assumed that both LDF parameters have the same value ($k_s = k_{s,1} = k_{s,2}$) to simplify the parameter estimation. The model was fitted to all the experimental data simultaneously by minimizing the sum of square residuals between the experimental and predicted data, using the delay time and the axial dispersion coefficient determined with the glass beads column. To take into account the presence of the 5 cm long glass beads section before the resin bed in the model, the bed length was set to 0.15 m, imposing the condition $N_i = 0$ for $z < 0.05$ m. The estimated value of k_s was

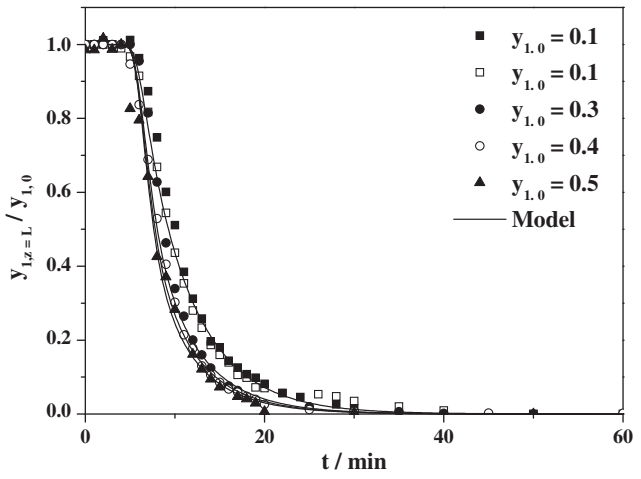

Fig. 5. Comparison between experimental and fitted ethanol desorption curves for several initial ethanol concentrations. $T = 308$ K, $Q_F = 1$ ml min^{-1}.

$(8.4 \pm 1.8)\ 10^{-3}\ s^{-1}$, with $r^2 = 0.985$. This value was used in the subsequent simulations. A comparison between the theoretical and the experimental desorption curves is given in Fig. 5. It is observed that the model reproduces the experimental desorption curves very well.

4.4. Model validation with rinse experiments

To study the model capability for describing the column dynamics in the separation of ethanol–water mixtures with Sepabeads 207® resin, the breakthrough curves predicted by the model were compared with the experimental breakthrough curves obtained in rinse experiments. Three rinse experiments were carried out in the same conditions (as described in the experimental section), and the comparison between the experimental and the predicted breakthrough curves are presented in Fig. 6. The average relative standard deviation of the measured ethanol mass fraction in these experiments was 1.85%.

No fitting parameters were used in this comparison. It can be observed that the model predicts reasonably well the breakthrough curve of the rinse experiments, where the ethanol concentration changes between 10% and 100%. The value of the used mass transfer parameter was estimated from experiments where ethanol concentration changes between 0% and 50%. Therefore, the model can be used to describe the column dynamics in the whole ethanol concentration range. As the developed model is based on conservation equations, it can be used to design the separation of ethanol–water liquid mixtures using columns of Sepabeads 207® resin taking into account the effect of the operating conditions on the process dynamics.

4.5. Design of a cyclic adsorption–desorption process for separating an ethanol–water mixture with columns of Sepabeads 207® resin

The multi-column cyclic adsorption–desorption process described in Fig. 7 is proposed for separating continuously an ethanol–water mixture. The process uses five identical adsorbent columns. The feed mixture is composed of ethanol and water only, with an ethanol content of 10% (w/w). It is assumed that the impurities accompanying this mixture in the fermentation broth have been removed, for example using a single distillation step. The energy requirement of this step is much lower than the one of a conventional distillation process for bioethanol production, because it is not necessary to get an ethanol-enriched distillate [21].

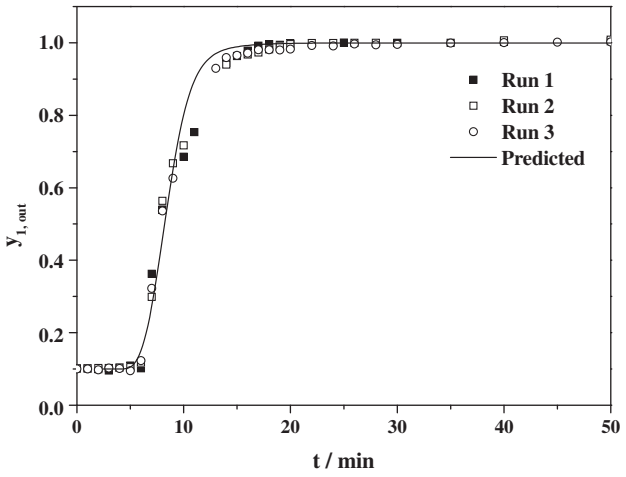

Fig. 6. Comparison between the predicted breakthrough curve and the experimental curves in three repeated rinse experiments. Conditions are described in the experimental section.

The cycle is composed of five consecutive stages where each column undergoes a different step with the same duration in the order: (1) Feed recovery, (2) Adsorption, (3) Rinse recovery, (4) Rinse, (5) Regeneration. All the stages are identical except for the column passing through each step in each stage. A similar cyclic process was proposed elsewhere for the separation of ethanol–water mixtures with silicalite as the adsorbent [23]. The process described here has two different features: (i) the regeneration does not require a previous cooling step before the adsorption step, as all the steps take place at 308 K, and (ii) a new feed recovery step must be included here because the mass transfer zone (MTZ) length of the adsorption step is quite longer than in the process with silicalite. The separation is based in the self-sharpening behavior of the column ethanol concentration profile when an ethanol-selective adsorbent is employed [32]. In these systems, when the adsorptive concentration decreases along the MTZ in the flow direction, the MTZ advancing along the column tends to reach a constant-pattern profile, with a constant length and constant velocity. Two different MTZ's appear in the proposed process, moving between two columns in the adsorption and feed recovery steps (MTZ1), and in the rinse and rinse recovery steps (MTZ2). If the column length is high enough, the MTZ's never reach the end of the second column. Thus, the MTZ's behave as if they moved along an infinitely long column. The cyclic steady-state is reached when the constant-pattern behavior is attained in all the columns. To design this process, it is necessary to calculate both MTZ1 and MTZ2 lengths, as well as their velocities. The column length must set to a value higher that the longer MTZ. The ratio between the feed flow rates in the adsorption and rinse steps must be manipulated to make the two MTZ's have the same velocity. The duration of each stage is the column length divided into this velocity.

To start the design, the column diameter and the feed flow rate of the rinse step are set to the values used in the experiments (1.05 cm and 1 ml min^{-1}). The column length is set to 1 m, after testing different values by trial and error. The rinse and rinse recovery steps in one stage are simulated simultaneously using a single column 2 m long, representing two 1 m columns connected in series. Both columns are initially saturated with a 10% ethanol–water mixture, and 100% ethanol is fed at $z = 0$ (inlet of the first column). The displacement of two reference concentration planes (with $y_1 = 0.995$ and $y_1 = 0.105$) is followed to analyze the movement of MTZ2 (Fig. 7). The stage duration has been manipulated until the plane with $y_1 = 0.995$ advances 1 m in the constant pattern conditions, resulting in 49.67 min. At the end of the stage, the ethanol and water concentration profiles are moved backwards (maintaining the attained shape), placing the plane with $y_1 = 0.995$ at $z = 0$. Then, the following stage is simulated, where both columns have initially the displaced concentration profiles of the previous stage. The variation of the length of MTZ2 as it advances in the direction of flow (following the movement of the plane with $y_1 = 0.995$, as it is depicted in Fig. 7), and the constant pattern concentration profiles are shown in Fig. 8.

The same method is used to design the feed recovery and adsorption steps. The stage duration is fixed to the one determined for the rinse and rinse recovery steps. In this case, the reference planes used to delimit MTZ1 are the ones with $y_1 = 0.095$ and $y_1 = 0.001$, and the simulation starts with both columns filled with water, feeding a 10% ethanol mixture at $z = 0$. The feed flow rate is manipulated until MTZ1 advances 1 m in one stage, resulting in 1.41 ml min^{-1}. Thus, the value of u_{MTZ} in Fig. 7 is 1 m/49.67 min = 0.0201 m min^{-1}. The constant pattern behavior is reached when the lengths of MTZ1 and MTZ2 are 0.93 and 0.64 m, respectively. The ratio between the lengths of MTZ1 and MTZ2 is about 1.4, which is very similar to the ratio of flow rates in the adsorption and rinse steps. This indicates that the main reason for the higher MTZ length in the adsorption step is the increase

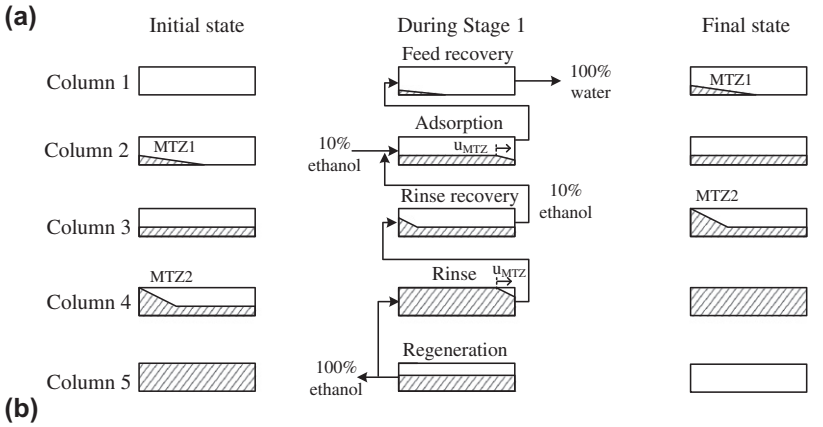

(b)

Column	Stage 1	Stage 2	Stage 3	Stage 4	Stage 5
1	Feed recovery	Adsorption	Rinse recovery	Rinse	Regeneration
2	Adsorption	Rinse recovery	Rinse	Regeneration	Feed recovery
3	Rinse recovery	Rinse	Regeneration	Feed recovery	Adsorption
4	Rinse	Regeneration	Feed recovery	Adsorption	Rinse recovery
5	Regeneration	Feed recovery	Adsorption	Rinse recovery	Rinse

Fig. 7. Scheme of a five-column cyclic adsorption–desorption process for separating continuously a 10% ethanol–water mixture. (a) Evolution of column concentration profiles in each stage. The velocity of MTZ1 and MTZ2 is u_{MTZ}. (b) Time schedule of the five columns in a cycle.

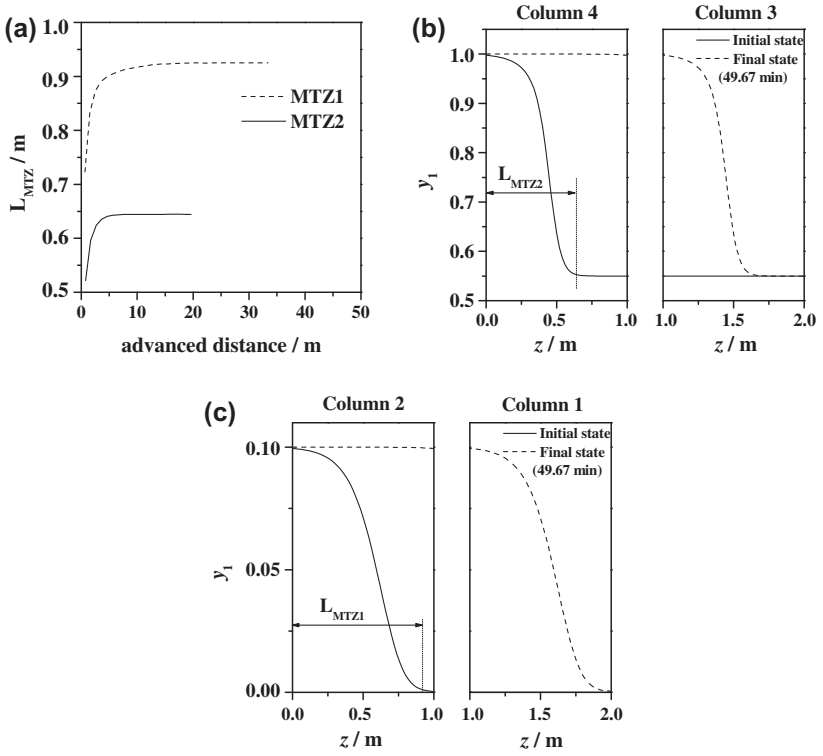

Fig. 8. Simulation results of the feed recovery and adsorption steps, and of the rinse recovery and rinse steps in the designed process. (a) Evolution of the MTZ length with the advanced distance. MTZ1 refers to the MTZ traveling between the adsorption and feed recovery steps, and MTZ2 refers to one traveling between the rinse and rinse recovery steps. (b) Ethanol concentration profiles in the rinse recovery and rinse steps when the constant-pattern behavior is attained. The column numbers refer to stage 1 in Fig. 7c ethanol concentration profiles in the feed recovery and adsorption steps when the constant-pattern behavior is attained.

of the mass transfer resistance control due to a shorter contact time (void volume/flow rate) in the column.

The MTZ length in the adsorption step determines the minimum allowable column size. To reduce the column size, it is necessary to use an adsorbent resulting in a shorter MTZ in this step. As the self-sharpening behavior increases with the favorable character of the ethanol adsorption isotherm [32] a resin with higher affinity towards ethanol in the low concentration range would result in a better performance (a shorter MTZ) with respect to Sepabeads 207® resin, providing that the rate of mass transfer between liquid and resin is similar.

The calculated lengths of MTZ1 and MTZ2 are both below the maximum allowable value (1 m). From this result, it is theoretically possible to separate a 10% ethanol–water mixture into its components with 100% recovery using 1 m long columns.

To estimate the specific production of ethanol per unit mass of adsorbent in this process, mass balances around one stage can be performed, since all the stages are equivalent. Mass balances

around three different sub-systems are considered: (1) the two columns undergoing the feed recovery and adsorption steps, (2) the two columns undergoing the rinse recovery and rinse steps, and (3) the column undergoing the regeneration step. The amounts of ethanol and water in the columns containing the MTZ's at the initial and final states (Fig. 7) can be disregarded in the mass balances around sub-systems (1) and (2), because they cancel with each other. It is deduced from the mass balances that the net ethanol product (in kg of ethanol per kg of resin) in the process is given by:

$$\text{Net ethanol product} = n_1(y_{1,F}) - n_2(y_{2,F})\frac{y_{1,F}}{y_{2,F}} \quad (24)$$

In the designed process, the net ethanol product is independent of the column length and the feed flow rates. This parameter not only depends on the ethanol column capacity. It also depends on the water column capacity, and it is strongly reduced if this capacity for the feed composition is very high. Eq. (24) shows that for evaluating the performance of any adsorbent in the separation of ethanol–water mixtures, the measurement of the column capacities of both ethanol and water is required. It is important to note that it is difficult to find data in the literature about water column capacities, particularly for polymeric resins. Introducing Eq. (21) and (22) in Eq. (24), the net ethanol product for a 10% ethanol feed is estimated as 0.11 kg kg^{-1}, which is higher than the value obtained with silicalite for the same feed ethanol concentration (0.073 kg kg^{-1}, [23]). Therefore, Sepabeads 207® resin presents good ethanol and water column capacities for the ethanol–water separation by adsorption.

5. Conclusions

Ethanol and water column capacities in Sepabeads 207® resin at 308 K have been measured. These data have been correlated to the ethanol and water liquid composition, in order to obtain expressions which can reproduce properly the experimental results. Also, it has been noticed that temperature, between 296 and 308 K, has a small effect on these column capacities. Sepabeads 207® resin can be considered as an ethanol-selective sorbent due to its higher affinity to ethanol in ethanol–water mixtures.

Mass transfer coefficients of ethanol and water have been calculated. By means of a sensitivity analysis, it has been concluded that water mass transfer coefficient has no significant effect compared to the one of ethanol mass transfer coefficient, so that the same value has been assumed for both. This assumption has been validated with the comparison between the experimental and theoretical data predicted by the model. In addition the model was validated with the experimental breakthrough curves obtained in rinse experiments. The model predicts well rinse experimental data in a wider concentration range.

The model has been used to design a cyclic adsorption–desorption process for separating an ethanol–water mixture with the proposed adsorbent. The process consists of five consecutive stages (feed recovery, adsorption, rinse recovery, rinse and regeneration), where each stage takes the same time. The calculated net ethanol product obtained for a 10% ethanol feed is higher than the one obtained in the same process using silicalite as adsorbent.

Acknowledgement

Financial support from the "Ministerio de Ciencia e Innovación" of Spain through project CTQ2009-08838 (PPQ) is gratefully acknowledged.

References

[1] K. Ramanathan, C.K. Koch, S.H. Oh, Kinetic modeling of hydrocarbon adsorbers for gasoline and ethanol fuels, Chem. Eng. J. 207–208 (2012) 175–194.
[2] S.C. Rabelo, H. Carrere, R.M. Filho, A.C. Costa, Production of bioethanol, methane and heat from sugarcane bagasse in a biorefinery concept, Bioresource Technol. 102 (2011) 7887–7895.
[3] S. González-García, D. Iribarren, A. Susmozas, J. Dufour, R.J. Murphy, Life cycle assessment of two alternative bioenergy systems involving *Salix* spp. biomass: bioethanol production and power generation, Appl. Energy 95 (2012) 111–122.
[4] N. Sarkar, S.K. Ghosh, S. Bannerjee, K. Aikat, Bioethanol production from agricultural wastes: an overview, Renew. Energy 37 (2012) 19–27.
[5] E. Martinez-Hernandez, J. Sadhukhan, G.M. Campbell, Integration of bioethanol as an in-process material in biorefineries using mass pinch analysis, Appl. Energy 104 (2013) 517–526.
[6] S.A. Leeper, P.C. Wankat, Gasohol production by extraction of ethanol from water using gasoline as solvent, Ind. Eng. Chem. Process Des. Dev. 21 (1982) 331–334.
[7] R.P. De Filippi, J.M. Moses, Extraction of organics from aqueous solutions using critical-fluid carbon dioxide, Biotechnol. Bioeng. Symp. 12 (1982) 205–219.
[8] M. Errico, B. Rong, Synthesis of new separation processes for bioethanol production by extractive distillation, Sep. Purif. Technol. 96 (2012) 58–67.
[9] N.B. Milestone, D.M. Bibby, Concentration of alcohols by adsorption on silicalite, J. Chem. Technol. Biotechnol. 31 (1981) 732–736.
[10] W.W. Pitt, G.L. Haag, D.D. Lee, Recovery of ethanol from fermentation broths using selective sorption–desorption, Biotechnol. Bioeng. 25 (1983) 123–131.
[11] S. Bui, X. Veryklos, R. Mutharasan, In situ removal of ethanol from fermentation broths. Selective adsorption characteristics, Ind. Eng. Chem. Process Des. Dev. 24 (1985) 1209–1213.
[12] M.B. Rao, S. Sircar, Production of motor fuel grade alcohol by concentration swing adsorption, Sep. Sci. Technol. 27 (1992) 1875–1887.
[13] T. Yamamoto, Y.H. Kim, B.C. Kim, A. Endo, N. Thongprachan, T. Ohmori, Adsorption characteristics of zeolites for dehydration of ethanol: evaluation of diffusivity of water in porous structure, Chem. Eng. J. 181–182 (2012) 443–448.
[14] M. Hashi, J. Thibault, F.H. Tezel, Recovery of ethanol from carbon dioxide stripped vapor mixture: adsorption prediction and modeling, Ind. Eng. Chem. Res. 49 (2010) 8733–8740.
[15] T. Ikegami, H. Yanagishita, D. Kitamoto, H. Negishi, K. Haraya, T. Sano, Concentration of fermented ethanol by pervaporation using silicalite membranes coated with silicone rubber, Desalination 149 (2002) 49–54.
[16] A. Verhoef, A. Figoli, B. Leen, B. Bettens, E. Drioli, B. Van der Bruggen, Performance of a nanofiltration membrane for removal of ethanol from aqueous solutions by pervaporation, Sep. Purif. Technol. 60 (2008) 54–63.
[17] S. Chovau, S. Gaykawad, A.J.J. Straathof, B. Van der Bruggen, Influence of fermentation by-products on the purification of ethanol from water using pervaporation, Bioresource Technol. 102 (2011) 1669–1674.
[18] E. Ivanova, M. Karsheva, Ethanol vapours adsorption by natural clynoptilolite, J. Univ. Chem. Technol. Metall. 42 (2007) 391–398.
[19] J. Jeong, H. Jeon, K. Ko, B. Chung, G. Choi, Production of anhydrous ethanol using various PSA (Pressure Swing Adsorption) processes in pilot plant, Renew. Energy 42 (2012) 41–45.
[20] F.A. Farhadpour, A. Bono, Sorptive separation of ethanol–water mixtures with a bi-dispersed hydrophobic molecular sieve, silicalite: measurement and theoretical analysis of column dynamics, Chem. Eng. Process 35 (1996) 157–168.
[21] S. Sircar, Process for Preparing Fuel Grade Alcohol, US patent 5,030,775, 1991.
[22] S. Sircar, M.B. Rao, Separation of Liquid Mixtures by Thermal Swing Adsorption, US patent 5,116,510, 1992.
[23] J.A. Delgado, M.A. Uguina, J.L. Sotelo, V.I. Águeda, A. García, A. Roldán, Separation of ethanol–water liquid mixtures by adsorption on silicalite, Chem. Eng. J. 180 (2012) 137–144.
[24] J.A. Delgado, M.A. Uguina, J.L. Sotelo, V.I. Águeda, P. Gómez, V. Hernández, Modeling the regeneration of a polymeric resin column saturated with ethanol by air purge and external heating, Sep. Sci. Technol. 46 (2011) 1740–1749.
[25] T.C. Bowen, L.M. Vane, Ethanol acetic acid and water adsorption from binary and ternary liquid mixtures on high-silica zeolites, Langmuir 22 (2006) 3721–3727.
[26] J.O. Maloney, Perry's Chemical Engineers' Handbook, eighth ed., McGraw-Hill, New York, 2008.
[27] Y.A. Cengel, M.A. Boles, Thermodynamics: An Engineering Approach, 3rd ed., McGraw-Hill, New York, 1998.
[28] N.K. Madsen, R.F. Sincovec, ALGORITHM 540 PDECOL, general collocation software for partial differential equations, ACM T. Math. Software 5 (1979) 326–351.
[29] G.F. Froment, K.B. Bischoff, Chemical Reactor Analysis and Design, second ed., Wiley, New York, 1990.
[30] A.D. McNaught, A. Wilkinson, IUPAC. Compendium of Chemical Terminology, second ed., Blackwell Scientific Publications, Oxford, 1997.
[31] R.T. Yang, Adsorbents: Fundamentals and Applications, New York, 2003.
[32] S. Sircar, M.B. Rao, Kinetics and column dynamics for adsorption of bulk liquid mixtures, AIChE J. 38 (1992) 811–820.